ELSEVIER

Chemical Engineering Journal 78 (2000) 13–19

Chemical Engineering Journal

www.elsevier.com/locate/cej

Application of the Danckwerts method in a bubble column Effects of surfactants on mass transfer coefficient and interfacial area

G. Vázquez [a], M.A. Cancela [a,*], C. Riverol [b], E. Alvarez [b], J.M. Navaza [a]

[a] *Department of Chemical Engineering, University of Santiago, 15706 Santiago, Spain*

[b] *Department of Chemical Engineering, University of Vigo, 36200 Vigo, Spain*

Received 28 January 1999; received in revised form 29 September 1999; accepted 5 October 1999

Abstract

We determined interfacial areas, A, and individual mass transfer coefficients, k_L, for the absorption of CO_2 in a bubble column, with an anionic surfactant in the absorbent liquid. The results of experiments to determine the dependence of k_L on surface tension of the liquid phase and the superficial velocity of the gas were fitted to within a 10% error by expressions of the form

$$k_L = K_4 \sigma^{1.35} u_G^{0.5}$$

where K_4 depends exclusively on the kind of bubbling device.

Likewise, the experimental values of specific area, a, were correlated with the column diameter d_c and the physical properties by means the following equation:

$$ad_c = K \cdot \mathrm{Re}^{0.98} \cdot \mathrm{Sc}^{0.57} \cdot \mathrm{Fr}^{0.09} \cdot \mathrm{Bo}^{-0.70} \left(\frac{d_p}{d_c}\right)^{-0.19}$$

that reproduces satisfactorily the experimental values.

Keywords: Danckwerts method; Interfacial area; Mass transfer coefficient; Surfactants

1. Introduction

Bubble columns are frequently used in the chemical industry as absorbers, fermenters and reactors in which heterogeneous gas–liquid or gas–solid reactions take place, in processes that require high contact areas between phases. They are particularly used with gas–liquid systems in which the liquid phase controls mass transfer, that is, the absorption of gases that are relatively insoluble [1]. In these columns, the gas is dispersed in the liquid phase in the form of small bubbles that provide high contact areas; mass transfer occurs during bubble formation and also during bubble rise.

Characteristic design criteria for this apparatus are: gas–liquid interfacial area, individual mass transfer coefficients, flow regime, bubble size distribution and coalescence of bubbles. Thus, most studies on bubble columns are devoted to the experimental determination of some of these parameters, and more specifically, of volumetric mass transfer coefficient. This parameter depends fundamentally on the gas flow and on the physical properties of the absorbent liquid. There are numerous correlations proposed for the superficial velocity of the gas as well as for the viscosity and surface tension of the liquid phase [2,3].

For absorption through a flat surface, the reduction of individual mass transfer coefficient, k_L, by use of a surfactant, whether due to hydrodynamic or barrier effects [4,5], can be offset by stirring [6], which renews the surface; but there are few quantitative data on the influence of surface tension on the volumetric mass transfer coefficient $k_L a$ when the gas to be absorbed is bubbled through the liquid phase. Since the presence of surfactants undoubtedly affects the formation and coalescence of bubbles, and hence the interfacial area, it is possible that surfactant-induced reduction of k_L due to barrier effects may be offset by increased area to afford increased values of $k_L a$ [7,8].

The volumetric mass transfer coefficient includes the specific gas–liquid area and the individual mass transfer

* Corresponding author. Present address: Departamento de Ingeniería Quimíca, Facultad de Ciencias, Campus universitario de Lugo, 27002 Lugo, Spain; Tel.: +34-8156-3100 x14216; fax: +34-8686-1143.
E-mail address: gelcan@usc.es (M.A. Cancela)

1385-8947/00/$ – see front matter
PII: S1385-8947(99)00174-6

coefficient, so to obtain the latter, it is necessary to first determine the interfacial area.

There are several methods for determining interfacial areas, the chemical methods are the most frequently used, the most common of these being the Danckwerts method, based on the absorption of CO_2 in sodium or potassium carbonate–bicarbonate buffer solutions. The application of this method requires the reaction to be first-order and moderately fast: the first condition is achieved working with a pH between 8 and 10, and the second using a catalyst. As proposed, catalysts are carbonic anhydrase [9,10], hypochlorite ions [11,12] sodium or potassium arsenite [13–15], the latter solute being the most commonly used.

In this work, we studied variations in gas–liquid interfacial area and individual mass transfer coefficient, determined by the Danckwerts method, with liquid phase surface tension and gas flow. We performed CO_2 absorption experiments in Na_2CO_3–$NaHCO_3$ (0.5–0.5 M) buffer solutions, in the presence of $NaAsO_2$ as catalyst; we used an anionic surfactant, sodium lauryl sulphate (SLS), to modify surface tension and analyze how it can influence the interfacial area and the individual mass transfer coefficient. Both parameters were correlated, individually and/or jointly, as a function of the surface rate of the gas and the surface tension of the liquid phase.

2. Theory

The chemical methods used to calculate interfacial area are based on the study of certain gas–liquid systems, and under specific conditions, absorption rate is directly proportional to the interfacial area. The method proposed by Danckwerts [13] requires that the gas absorbed undergoes a moderately fast pseudo-first-order reaction with some of the solutes in the liquid phase. Under these conditions, the absorption rate is given by

$$n = C^{e} A \sqrt{k_L^2 + k_1 D} \quad (1)$$

with n being the absorption rate, $\mathrm{mol\,s^{-1}}$; A the effective interfacial area, $\mathrm{m^2}$; C^e the gas solubility, $\mathrm{mol\,l^{-1}}$; D the gas diffusivity, $\mathrm{m^2\,s^{-1}}$; k_L the mass transfer individual coefficient, $\mathrm{m\,s^{-1}}$; k_1 the kinetic coefficient of the pseudo-first-order reaction, $\mathrm{s^{-1}}$.

The value A is obtained from the slope of the straight line that results from the graphical plot of N^2 versus k_1, while the value k_L is calculated from the ordinate at the origin.

Under certain conditions, CO_2 reaction in carbonate–bicarbonate buffer solutions catalyzed by sodium or potassium arsenite can be considered pseudo-first-order. In this case, dissolved CO_2 reacts with hydroxyl ions and water, this last reaction being catalyzed by arsenite ions, to give the global reaction

$$CO_2 + CO_3^{=} + H_2O \rightarrow 2HCO_3^{-}$$

For the reaction to be pseudo-first-order, it is necessary that $CO_3^{=}$, HCO_3^{-} and O^{-} ion concentrations remain constant, without decreasing near the interface. For this, the following condition must be fulfilled [16]:

$$C^{e} = \left[\frac{1}{[CO_3^{=}]} + \frac{2}{[HCO_3^{-}]}\right]\left[\sqrt{1 + \frac{Dk_1}{K_L^2}} - 1\right] \ll 1 \quad (2)$$

The kinetics coefficient of the global process, k_1, is being given by

$$k_1 = k_{H_2O} + k_{OH^-}[OH^-] + k_c[Cat] = k_0 + k_c[Cat] \quad (3)$$

where k_0 and k_c are the contributions of the not catalyzed and catalyzed reactions, respectively, and [Cat] represents the concentration of the catalyst, that is, the arsenite ion.

Under our working conditions, coefficients k_0 and k_c are $0.86\,\mathrm{s^{-1}}$ and $350\,\mathrm{l\ ion\,g^{-1}\,s^{-1}}$, respectively [16,17]; thus, the global kinetic coefficient is expressed as

$$k_1 = 0.86 + 350[AsO_2^{-}] \quad (4)$$

This method has the advantage that appreciable differences of k_1 are obtained using very small catalyst concentrations, thereby, not affecting the physical properties of the absorbent.

3. Materials and methods

3.1. Mass transfer measurements

Mass transfer measurements were carried out using the apparatus shown in Fig. 1. Except for the contact device, this setup has been described in detail in previous papers [18].

A bubble column (1) was used as contact device in this work, made of two methacrylate concentric cylindrical tubes, 108.6 cm high and 4 mm thick, welded to two flat bases made of the same material. The internal and external diameters of the column are 11.3 and 14.8 cm, respectively. On the external tube, there are two side orifices for the inward and outward flow of the thermostated liquid which circulates throughout the empty space between the two tubes.

The upper cover of the column, that easily comes apart, is a methacrylate sheet with three openings; the center orifice is for a thermometer (2), and the two off-centre orifices are for the inflow of liquid (3), and the outflow of gas (4), respectively. The lower cover also possesses three openings: the middle one is for a porous plate of 4 cm in diameter (5), and the outer ones are for a thermometer (6), and the outflow of liquid (7). The liquid enters the column through the top sheet, via a vertical glass tube that is slightly bent at the lower end to avoid gas leakage, while the gas inlet is through a porous plate. Bubble size is varied using three porous plates (the pore sizes of the plates used in this work are listed in Table 1).

The liquid phases used in this work (sodium carbonate–bicarbonate (0.5–0.5 M) buffer solutions with sodium

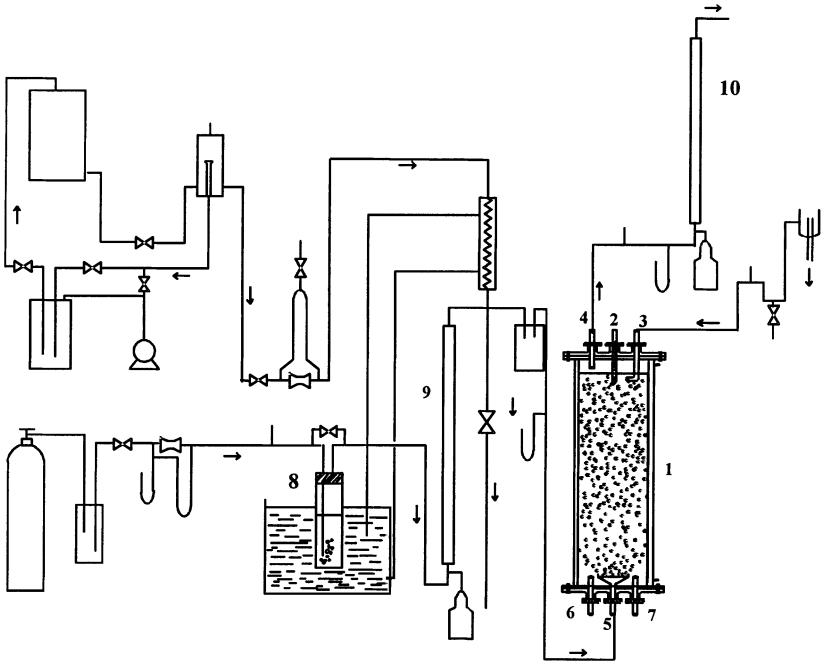

Fig. 1. Experimental setup for gas absorption measurements.

arsenite, as catalyst, and with SLS) were thermostated to 25°C before entering the contact device. For batch runs, the liquid load was 10.3 l. The concentration ranges used are $0–10^{-2}$ mol l^{-1} for sodium arsenite, and $0–5\times10^{-4}$ mass%, for SLS.

The gas to be absorbed, pure CO_2, was passed through a humidifier at 25°C (8) and it entered the contact device at a constant flow rate measured with a bubble flowmeter (9). Gas outflow through the top-plate outflow port was measured with another bubble flowmeter (10) before its release into the atmosphere. The gas absorption rate was calculated as the difference between inflow and outflow rates. In our experiments, we used inflow between 3 and 8.5×10^{-4} mol s^{-1}.

3.2. Physical properties

Interpretation and correlation of the mass transfer data obtained require knowledge of the densities, viscosities and surface tension of the liquid phases used, and the solubilities and diffusivities of the gas in these phases.

The densities and viscosities of the sodium carbonate–bicarbonate buffer solutions, with surfactant and sodium arsenite, were measured at 25°C using Gay–Lussac-type pycnometers of 25 cm^3 and a Schott Geräte AVS 350 automatic Ubbelohde viscometer, respectively. However, neither of these properties differed significantly from the values for the buffer solutions, ρ=1075.1 kg m^{-3} and $\mu=1.31\times10^{-3}$ kg m^{-1} s^{-1}.

The surface tension, σ, of the liquid phase changes notably with surfactant addition (see Table 2), thus having necessarily to be precisely measured. In view of the scarceness of data in the literature, we have proceeded to its experimental determination using a stalagmometer previously calibrated with distilled and deionized water. The surface tension of water was determined with a Prolabo tensiometer and its value differs by less than 0.07% of that found in the literature [19]. The temperature of the solution was held constant by placing it in a container equipped with an isothermal jacket, and was controlled with a precision of ±0.02 K.

The solubilities and diffusivities of CO_2 in the buffer solutions with SLS were calculated from the correlation equations found in the literature [20–22]. Since the addition of SLS did not modify the viscosity of the solution, the diffusivity and the solubility of CO_2 were also assumed equal to their values for buffer solutions. Diffusivity, *D*, was calculated from the expression proposed by Joosten and

Table 1
Equivalent pore size ranges of the bubbling plates used

Plate	Equivalent pore diameter$\times10^6$ (m)
0	150–200
1	90–150
2	40–90

Table 2
Surface tension of the different solutions at 25°C

[SLS]$\times10^5$ (mass%)	$\sigma\times10^3$ (N m^{-1})
0	75.01
5	74.42
10	71.06
50	65.96

Danckwerts [20]:

$$\frac{D}{D_d} = \left(\frac{\mu_d}{\mu}\right)^{\alpha} \quad (5)$$

where μ and μ_d are the viscosities of the buffer solution and of the solvent (water), respectively, α is a parameter whose value for solutions of this nature is 0.82 and D_d is the diffusivity of CO_2 in water, which was calculated from the equation of Wilke and Chang [21].

The solubility of CO_2 in buffer solutions with SLS and/or sodium arsenite, due to the electrolytic nature of these, was calculated from the equation proposed by Danckwerts and Gillham [22] for solutions containing more than one electrolyte:

$$\log\left(\frac{C^e}{C_d^e}\right) = -\sum_i K_{si} I_i \quad (6)$$

where I_i and K_{si} are the ionic strength and the salting out parameter for each electrolyte and C_d^e is the solubility of CO_2 in the solvent. The values of K_{si} for Na_2CO_3 and $NaHCO_3$ are 0.097 and 0.199, respectively.

It was proved that the addition of sodium arsenite does not affect either the diffusivity or the solubility of CO_2, due to its low concentration. Therefore, the diffusivity and the solubility of CO_2 will be considered constant for all the buffer solutions used and equal to $1.54\times10^{-9}\,m^2\,s^{-1}$ and $1.925\times10^{-2}\,mol\,l^{-1}$, respectively.

4. Results and discussion

The amount of CO_2 absorbed per unit volume and time, N, depends on gas flow rate, pore size, and catalyst and surfactant concentrations, as shown in Fig. 2 for one of the systems tested. In Fig. 2, we observe that N increases with

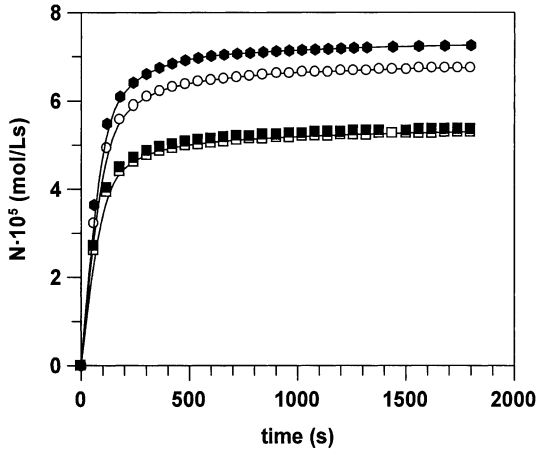

Fig. 2. Time-dependence of N for different gas flow rates and surfactant concentrations: plate 0 and without SLS, in Danckwerts method. (●) $0.0008\,mol\,s^{-1}$ and [sodium arsenite]$=4\times10^{-3}$ M; (○) $0.0008\,mol\,s^{-1}$ and [sodium arsenite]$=0$ M; (■) $0.0059\,mol\,s^{-1}$ and [sodium arsenite]$=4\times10^{-3}$ M; (□) $0.0059\,mol\,s^{-1}$ and [sodium arsenite]$=0$ M.

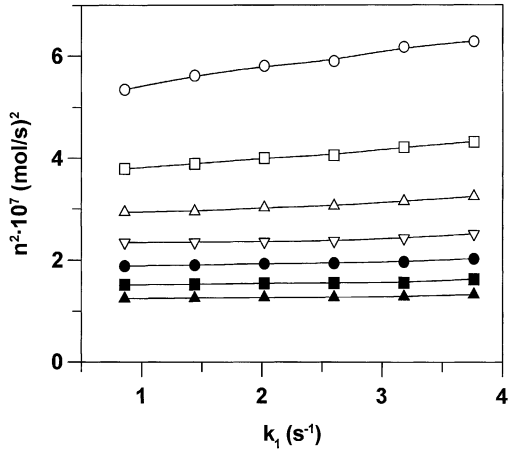

Fig. 3. Danckwerts plots, plate 0 and different gas flow rates. (○) $8.1\times10^{-4}\,mol\,s^{-1}$, (□) $6.7\times10^{-4}\,mol\,s^{-1}$, (△) $5.8\times10^{-4}\,mol\,s^{-1}$, (▽) $5.1\times10^{-4}\,mol\,s^{-1}$, (●) $4.6\times10^{-4}\,mol\,s^{-1}$, (■) $4.1\times10^{-4}\,mol\,s^{-1}$ (▲) $3.1\times1^{-4}\,mol\,s^{-1}$.

the gas flow rate and with the concentration of catalyst, for a given pore size and SLS concentration.

When the amount of CO_2 absorbed is evaluated, the Danckwerts method is applied to determine the interfacial area, A, and the individual mass transfer coefficient, k_L. In accord with the method of Danckwerts, Fig. 3 shows n^2 plotted versus k_1 (Eq. (1)) for one of the SLS concentrations and for different gas flow rates. The interfacial areas were calculated from the slopes of the resulting lines, and the values of the corresponding mass transfer coefficients from the intercepts.

For the calculated values of A and k_L, we observe a decrease with the concentration of SLS, that is, as the surface tension decreases. The reduction may be attributed to the effect of the surface agents, since they reduce interfacial movements because they occupy part of the surface of the bubbles. The surface concentration of surfactant increases with the surfactant concentration in the liquid bulk and as the surface tension decreases [23]. In systems with intense coalescence rate, the area can be considerably modified with respect to the expected area as a function of bubble size and gas flow. However, for systems with high viscosity, coalescence decreases, and for a given gas flow, the effective area is modified with the concentration of the surface agent [24].

The individual mass transfer coefficients have been correlated, individually and globally, with superficial gas velocity and with surface tension, to quantify the effect of these variables. We have first studied the influence of superficial gas velocity, u_G, over the individual mass transfer coefficient for each concentration of SLS (Fig. 4). This influence has been quantified, giving an expression that is similar to that proposed by Sotelo [2]:

$$k_L = K_2\, u_G^{0.5} \quad (7)$$

with the empirically determined values of K_2 listed in Table 3. The values of K_2 decreased with increasing

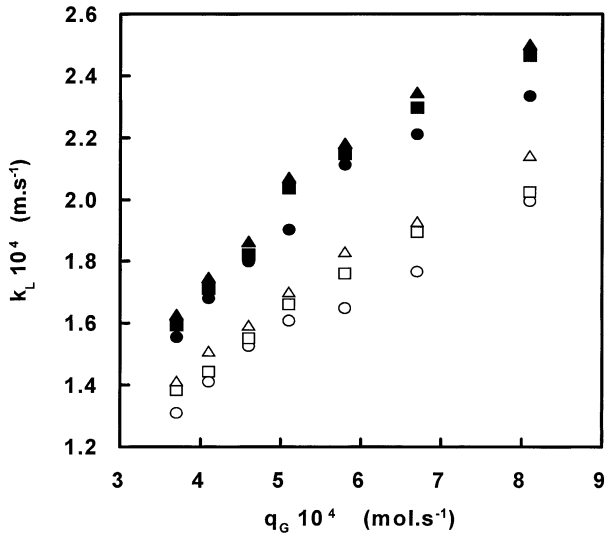

Fig. 4. Dependence of the individual mass transfer coefficient k_L on the gas flow rate. (●) without SLS and plate 0, (■) without SLS and plate 1, (▲) without SLS and plate 2, (○) [SLS]=5×10^{-4} mass% and plate 0, (□) [SLS]=5×10^{-4} mass% and plate 1, (Δ) [SLS]=5×10^{-4} mass% and plate 2.

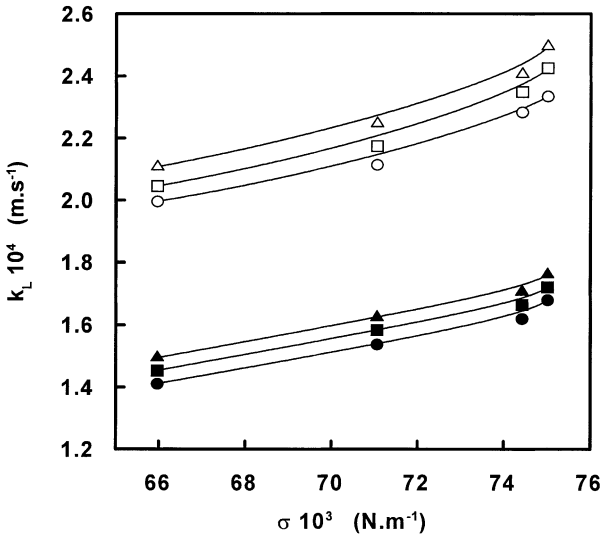

Fig. 5. Dependence of the individual mass transfer coefficient k_L on surface tension. [SLS]=10^{-4} mass%. (●) 4.1×10^{-4} mol s^{-1} and plate 0, (■) 4.1×10^{-4} mol s^{-1} and plate 1, (▲) 4.1×10^{-4} mol s^{-1} and plate 2, (○) 8.1×10^{-4} mol s^{-1} and plate 0, (□) 8.1×10^{-4} mol s^{-1} and plate 1, (Δ) 8.1×10 mol s^{-1} and plate 2.

surfactant concentration and with increasing bubble-plate pore size (see Fig. 4).

There is an obvious dependence between of the individual mass transfer coefficient and surface tension in solutions that contain surfactants as seen in Fig. 5. When analyzing the influence of surface tension, in an individualized way, we obtain the following expression:

$$k_L = K_3 \sigma^{1.35} \quad (8)$$

in which K_3 is a function of the superficial gas rate and bubble-plate pore size (Table 4). The values of K_3 increased with increasing gas flow rate and with decreasing bubble-plate pore size (see Fig. 5). We can conclude that the influence of pore size is lower than that of gas flow, since the value of the parameter oscillates considerably with gas flow.

The joint analysis of the dependence of k_L with the surface rate of the gas and with the surface tension leads to an expression in the form

$$k_L = K_4 \sigma^{1.35} u_G^{0.5} \quad (9)$$

where the parameter K_4 depends exclusively on the bubble-plate pore size and its values are shown in Table 5.

Table 3
Values of the parameter K_2 in Eq. (7)

[SLS] (mass%)	$K_2\times10^3$ ($m^{0.5}\,s^{0.5}$)		
	Plate 0	Plate 1	Plate 2
0	5.4761	5.7127	5.8041
5×10^{-5}	5.1325	5.3074	5.4585
1×10^{-4}	4.8749	5.0480	5.1837
5×10^{-4}	4.5541	4.7024	4.8493

Table 4
Values of the parameter K_3 in Eq. (8)

$u_G\times10^3$ (m s^{-1})	$K_3\times10^2$ (m s$^{1.70}$ kg$^{-1.35}$)		
	Plate 0	Plate 1	Plate 2
1.81	7.5489	7.7956	8.0555
1.53	6.7121	7.0416	7.1957
1.33	6.4343	6.6447	6.7899
1.17	5.9708	6.2990	6.4478
1.05	5.8340	5.9843	6.0983
0.95	5.4838	5.6337	5.7831
0.87	5.1175	5.2716	5.4056

If we consider a single value for this parameter, we would make an error of 6%.

In Fig. 6, the experimental values of k_L and those calculated from Eq. (9) are compared, for one of the porous plates employed. The deviation between both values is, in all cases, less than 10%.

On the other hand, the experimental interfacial areas vary with gas flow rate in a linear dependence; this behaviour is similar to that observed for all plates (Fig. 7). The dependence of area with surface tension is a non-linear relation; interfacial area decreases with increasing surfactant concentration, that is, when the surface tension decreases. This

Table 5
Values of the parameter K_4 in Eq. (9)

	K_4 ($m^{0.5}\,s^{22}\,kg^{-1.35}$)
Plate 0	0.17587
Plate 1	0.18233
Plate 2	0.18689

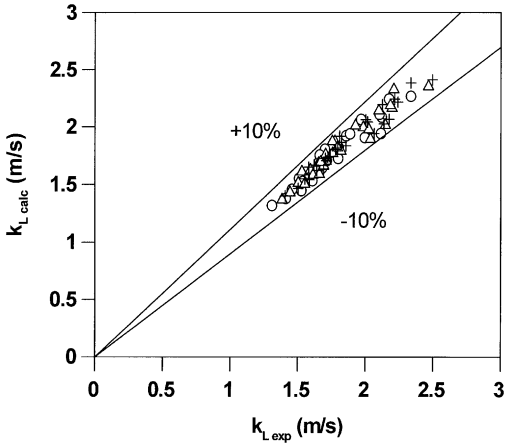

Fig. 6. k_L calculated with Eq. (9) vs. experimental k_L, for two porous plates and different gas flow rates. (○) plate 0; (Δ) plate 1; (+) plate 2.

behaviour is due to the fact that the presence of surfactant in the medium reduces turbulence; the relation between both variables can be quantified by the exponent 0.7. In Fig. 8, we observe the influence of this variable over area.

At last, an analysis of specific area, a, was carried out as a function of the dimensionless modules, affording the following equation:

$$ad_c = K_5 \cdot \mathrm{Re}^{0.98} \cdot \mathrm{Sc}^{0.57} \cdot \mathrm{Fr}^{0.09} \cdot \mathrm{Bo}^{-0.70} \left(\frac{d_p}{d_c}\right)^{-0.19} \quad (10)$$

It is worth pointing out that, for the first term, instead of introducing the interfacial area, we use the product of specific area by the diameter of the column that is a dimensionless product. Bo, Fr, Re and Sc are the modules of Bond, Froud,

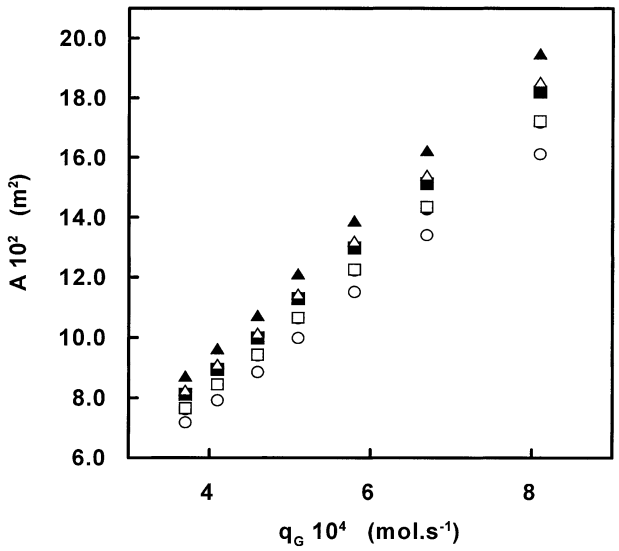

Fig. 7. Dependence of interfacial area on the gas flow rate. (●) without SLS and plate 0, (■) without SLS and plate 1, (▲) without SLS and plate 2, (○) [SLS]=1×10^{-4} mass% and plate 0, (□) [SLS]=1×10^{-4} mass% and plate 1, (Δ) [SLS]=1×10^{-4} mass% and plate 2.

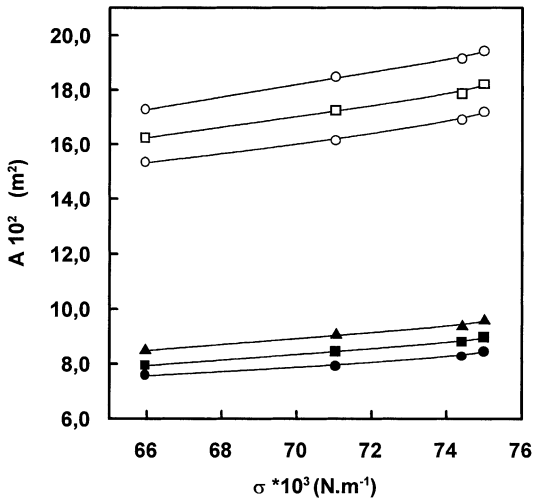

Fig. 8. Dependence of interfacial area on surface tension. (●) 4.1×10^{-4} mol s^{-1} and plate 0, (■) 4.1×10^{-4} mol s^{-1} and plate 1, (▲) 4.1×10^{-4} mol s^{-1} and plate 2, (○) 8.1×10^{-4} mol s^{-1} and plate 0, (□) 8.1×10^{-4} mol s^{-1} and plate 1, (Δ) 8.1×10^{-4} mol s^{-1} and plate 2.

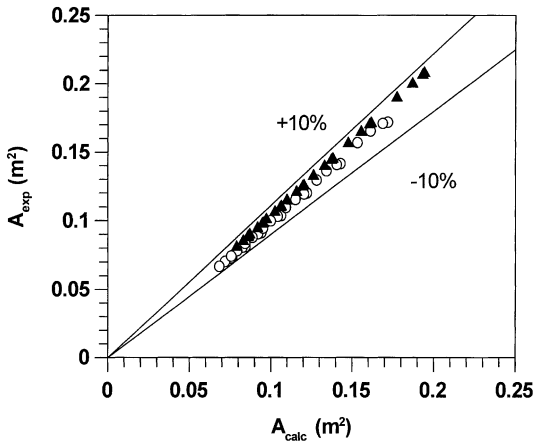

Fig. 9. Experimental interfacial areas vs. calculated values (Eq. (10)), for different SLS solutions and two porous plates: (○) plate 0, (▲) plate 2.

Reynolds, and Schmidt, respectively, d_p and d_c are the pore diameter and the column diameter, respectively, and K_5 is an adjustment parameter of value 4.8×10^{-2}. Fig. 9 shows, for one of the porous plates, the value of the experimental area versus the calculated one (Eq. (10)), the deviations always being lower than 10%.

5. Conclusions

In view of our results, we can conclude that, in the systems tested, the presence of the surfactant induces reduction of the interfacial area as well as of the individual transfer coefficient, and that both increase with gas flow rate, and decrease with increasing bubble-plate pore size.

6. Notation

a	specific area (m^{-1})
A	effective interfacial area (m^2)
C^e	gas solubility ($mol\,l^{-1}$)
C_d^e	gas solubility in the bulk liquid ($mol\,l^{-1}$)
d_c	column diameter (m)
d_p	pore diameter (m)
D	gas diffusivity ($m^2\,s^{-1}$)
D_d	gas diffusivity in the bulk liquid ($m^2\,s^{-1}$)
g	gravitational acceleration ($m\,s^{-2}$)
I_i	ionic strength of the electrolyte i
k_L	mass transfer individual coefficient ($m\,s^{-1}$)
k_1	kinetic coefficient (s^{-1})
K_1	salting-out parameter of electrolyte i
K_2	parameter in Eq. (7) ($m^{0.5}\,s^{-0.5}$)
K_3	parameter in Eq. (8) ($m\,s^{1.70}\,kg^{-1.35}$)
K_4	parameter in Eq. (9) ($m^{0.5}\,s^{2.2}\,kg^{-1.35}$)
K_5	parameter in Eq. (10)
n	absorption rate ($mol\,s^{-1}$)
N	absorption rate per unit volume ($mol\,l^{-1}\,s$)
q_g	gas flow rate ($mol\,s^{-1}$)
u_G	superficial gas velocity ($m\,s^{-1}$)

Greek symbols

α	parameter in Eq. (5)
μ	buffer solution viscosity ($kg\,m^{-1}\,s^{-1}$)
μ_d	viscosity of the solvent ($kg\,m^{-1}\,s^{-1}$)
ρ	density ($kg\,m^{-3}$)
σ	surface tension ($N\,m^{-1}$)

Dimensionless modules

Bo	Bond number ($g\,d^2\,\rho/\sigma$)
Fr	Froud number (u_G^2/dg)
Re	Reynolds number ($\rho\,u_G^2\,d/\mu$)
Sc	Schmidt number ($\mu/\rho D$)

References

[1] J.R. Welty, Fundamentals of Momentum, Heat and Mass Transfer, 3rd Edition, Wiley, New York, 1983.

[2] J.L. Sotelo, F.J. Benitez, L. Cabrera, Liquid mass transfer in laminar flow in a column containing a string of spheres and cylinders, Can. J. Chem. Eng. 63 (1986) 233–236.

[3] J.L. Sotelo, F.J. Benitez, J. Beltrán-Heredia, C. Rodríguez, Gas hold-up and mass transfer coefficients in bubble columns, Int. Chem. Eng. 34 (1994) 83–87.

[4] H. Yagi, F. Yoshida, Oxygen absorption in fermenters. Effects of surfactants, antifoaming agents and sterilized cells, J. Ferment. Technol. 52 (1974) 905–916.

[5] G. Vazquez, G. Antorrena, J.M. Navaza, V. Santos, Absorption of CO_2 by water and surfactant solutions in the presence of induced marangoni effect, Chem. Eng. Sci. 51 (1996) 3317–3324.

[6] J. Llorens, C. Mans, J. Costa, Discrimination of the effects of surfactants in gas absorption, Chem. Eng. Sci. 43 (1988) 443–450.

[7] R.S. Albal, Y.T. Shah, A. Schumpe, Mass transfer in multiphase agitated contactors, Chem. Eng. J. 27 (1983) 61–80.

[8] Y. Kawase, M. Moo-Young, Volumetric mass transfer coefficients in areated stirred tank reactors with Newtonian and non-Newtonian media, Chem. Eng. Res. Dev. 66 (1988) 284–288.

[9] D.N. Dean, M.J. Fuchs, J.M. Schaffer, R.G. Carbonell, Batch absorption of CO_2 by ree and microencapsulated carbonic anhydrase, Ind. Eng. Chem. Fundam. 16 (1977) 452–458.

[10] E. Alper, W.D. Deckwer, Kinetics of absorption of CO_2 into buffer solutions containing carbonic anhydrase, Chem. Eng. Sci. 35 (1980) 549–557.

[11] M.M. Sharma, P.V. Danckwerts, Catalysis by Brönsted bases of the reaction between CO_2 and water, Trans. Faraday Soc. 59 (1963) 386–395.

[12] R. Pohorecki, The absorption of CO_2 in carbonate–bicarbonate buffer solutions containing hypochlorite of catalyst on a sieve plate, Chem. Eng. Sci. 13 (1968) 1447–1451.

[13] D. Roberts, P.V. Danckwerts, Kinetics of CO_2 absorption in alkaline solutions I. Transient absorption rates and catalysis by arsenite, Chem. Eng. Sci. 17 (1962) 961–993.

[14] G. Astarita, D.W. Savage, J.M. Longo, Promotion of CO_2 mass transfer in carbonate solutions, Chem. Eng. Sci. 36 (1981) 581–588.

[15] C. Giavarini, M. Moresi, Absorption of CO_2 in aqueous solutions: screening of catalysts for potassium carbonate solutions, Ing. Chim. Ital. 17 (1981) 21–26.

[16] P.V. Danckwerts, M.M. Sharma, The absorption of carbon dioxide into solutions of alkalis and amines, Chem. Eng. J. 44 (1966) CE244.

[17] E. Alper, W.D. Deckwer, P.V. Danckwerts, Comparison of effective interfacial areas with the actual contact area for gas absorption in a stirred cell, Chem. Eng. Sci. 35 (1980) 1263–1268.

[18] G. Vázquez, G. Antorrena, J.M. Navaza, V. Santos, T. Rodríguez, Absorption of CO_2 in aqueous solutions of various viscosities in the presence of induced turbulence, Int. Chem. Eng. 33 (1993) 649–655.

[19] R.C. Weast, Handbook of Chemistry and Physics, 67th Edition, Chem. Rubber Pub. Co., Cleveland, 1987.

[20] G.E. Joosten, P.V. Danckwerts, Solubility and diffusivity of nitrous oxide in equimolecular potassium carbonate–potassium bicarbonate solutions at 25°C and 1 atm, J. Chem. Eng. Data 17 (1972) 452–454.

[21] C.R. Wilke, P. Chang, Correlation of diffusion coefficients in dilute solutions, AIChE J. 1 (1955) 264–270.

[22] P.V. Danckwerts, A.J. Gillham, The design of gas absorbers I. Methods for predicting rates of absorption with chemical reaction in packed columns and tests with 1(1/2)-inch Raschig rings, Trans. Inst. Chem. Eng. 44 (1966) 42–54.

[23] G. Vázquez, M.A. Cancela, R. Varela, E. Alvarez, J.M. Navaza, Influence of surfactants on absorption of CO_2 in a stirred tank with and without bubbling, Chem. Eng. J. 67 (1997) 131–137.

[24] M. Nocentini, D. Fajner, G. Pasquali, F. Magelli, Gas liquid mass transfer and hold-up in vessels stirred with multiple Rusthon turbines: water and water–glycerol solutions, Ind. Chem. Eng. Res. 32 (1993) 19–30.